

## Supplementary Information

### **Increasing the redox switching capacity of Lindqvist-type hexavanadates by organogold post-functionalisation**

Stanislav K. Petrovskii,<sup>a</sup> Marco Moors,<sup>a</sup> Sebastian Schmitz,<sup>a</sup> Elena V. Grachova\*<sup>b</sup> and Kirill Yu. Monakhov\*<sup>a</sup>

<sup>a</sup> *Leibniz Institute of Surface Engineering (IOM), 04318 Leipzig, Germany*

<sup>b</sup> *Institute of Chemistry, St Petersburg University, 198504 St. Petersburg, Russia*

Correspondence [kirill.monakhov@iom-leipzig.de](mailto:kirill.monakhov@iom-leipzig.de), [e.grachova@spbu.ru](mailto:e.grachova@spbu.ru)

## Content

Experimental details.....	4
Materials and instruments .....	4
Synthesis of POV precursor.....	4
Synthesis of {V <sub>6</sub> }-organogold hybrids .....	5
STM/STS measurements and sample preparation .....	6
<b>Figure S1.</b> The structures of compounds <b>1–4</b> (NBu <sub>4</sub> <sup>+</sup> cations omitted for clarity). .....	6
<b>Figure S2.</b> <sup>1</sup> H NMR (top) and <sup>1</sup> H- <sup>1</sup> H COSY NMR (aromatic region, bottom) spectra of hybrid <b>2</b> . ....	7
<b>Figure S3.</b> <sup>1</sup> H NMR (top), <sup>1</sup> H- <sup>1</sup> H COSY NMR (aromatic region, bottom left) and <sup>31</sup> P NMR (bottom right) of hybrid <b>3</b> . .....	8
<b>Figure S4.</b> <sup>1</sup> H NMR (top), <sup>1</sup> H- <sup>1</sup> H COSY NMR (aromatic region, bottom left) and <sup>31</sup> P NMR (bottom right) of hybrid <b>4</b> . .....	9
<b>Figure S5.</b> ESI-MS of {V <sub>6</sub> }-Au: experimental spectrum and simulated isotopic patterns for the dominating signals. ....	10
<b>Figure S6.</b> FTIR spectra of hybrids {V <sub>6</sub> }-Au and {V <sub>6</sub> }-N <sub>3</sub> in the fingerprint region, KBr.....	11
<b>Figure S7.</b> UV-vis absorption spectra of the hybrids <b>1–4</b> and {V <sub>6</sub> }-N <sub>3</sub> (for comparison) in 10 <sup>-5</sup> M CH <sub>2</sub> Cl <sub>2</sub> solutions. ....	11
<b>Table S1.</b> Binding energy of element signals observed in XPS spectra of <b>1, 3</b> and <b>4</b> . ....	12
<b>Figure S8.</b> Photoemission core-level N 1s, P 2p, O 1s and V 2p spectra taken from freshly deposited molecular layers of complex <b>1</b> on Au(111). ....	12
<b>Figure S9.</b> Photoemission core-level N 1s, S 2p, O 1s and V 2p spectra taken from freshly deposited molecular layers of complex <b>3</b> on Au(111), and P 2p on Si. ....	12
<b>Figure S10.</b> Photoemission core-level N 1s, P 2p, S 2p, O 1s and V 2p spectra taken from freshly deposited molecular layers of complex <b>4</b> on Au(111). ....	13
<b>Figure S11.</b> STM images of the samples obtained by drop casting deposition of 10 <sup>-5</sup> M MeCN and CH <sub>2</sub> Cl <sub>2</sub> solutions of <b>1–4</b> on Au(111). ....	14
<b>Figure S12.</b> Particle size distribution observed at different U <sub>B</sub> values for the selected area of the samples obtained by drop casting deposition of <b>1</b> onto the Au(111) surface .....	15
<b>Figure S13.</b> Particle size distribution observed at different U <sub>B</sub> values for the selected area of the samples obtained by drop casting deposition of <b>3</b> onto the Au(111) surface .....	16

<b>Figure S14.</b> Particle size distribution observed at different $U_B$ values for the selected area of the samples obtained by drop casting deposition of <b>4</b> onto the Au(111) surface .....	17
<b>Figure S15.</b> Subsequent STM scans for compounds <b>1</b> , <b>3</b> , and <b>4</b> . .....	18
<b>Figure S16.</b> STM image of <b>4</b> on Au(111) observed at bias voltage +2 V. Cross-section of one particle and schematic representation of possible charge distribution.....	19
<b>Figure S17.</b> STS $I(V)$ curves (dashed) and derivative $dI/dV$ (solid) curves for single molecules of <b>3</b> (left) and <b>4</b> (right) on Au(111). The very poor data convergency for <b>3</b> illustrates destabilization of its reduced states on Au(111).....	19
References.....	20

## Experimental details

### Materials and instruments

All synthetic manipulations were carried out under argon using standard Schleck technique. UWave 2000 reactor was used to carry out microwave assisted click-reactions. Starting materials were used from commercial sources as received. All solvents used for the synthesis were purified according to literature protocols.<sup>1</sup> The solution  $^1\text{H}$ ,  $^{13}\text{C}\{^1\text{H}\}$ ,  $^{31}\text{P}\{^1\text{H}\}$  and  $^{51}\text{V}$  NMR spectra were recorded on a Bruker 400 MHz Avance spectrometer. Mass spectra were measured on a LC/MS hybrid ultrahigh resolution electrospray quadrupole time-of-flight (UHR ESI-q-TOF) mass spectrometer Bruker MaXis 4G in the ESI negative mode. Fourier transform infrared spectra (FTIR) were measured on a Shimadzu IRAffinity spectrometer in KBr pellets. UV/Vis absorption spectra were measured using Shimadzu UV-1800 spectrometer in 1 cm quartz cuvettes.

A Thermo Scientific ESCALAB 250Xi system with an AlK $\alpha$  X-ray source was used to record X-ray photoelectron spectroscopy (XPS) spectra. Sub-monolayer thin films of **1**, **3** and **4** were prepared on Au(111) (A Si wafer was used to measure P 2p spectrum for **3**) in air by droplet deposition of the  $10^{-5}$  M dichloromethane solutions.

The carbene ligand precursor 1,3-diisopropyl-1H-benzimidazolium chloride (**iPr** $\cdot$ HCl) was prepared according to the literature protocol.<sup>2</sup> Terminal acetylenes 2-ethynylthiophene and 2-(4-ethynylphenyl)thiophene were obtained from the corresponding bromide derivatives by Sonogashira coupling reactions.<sup>3</sup>

[Au(tht)Cl] was synthesised according to a published method.<sup>4</sup> Gold(I) phosphine chloride complex [(MeO(C<sub>6</sub>H<sub>4</sub>))<sub>3</sub>P–AuCl] was prepared according to a conventional procedure.<sup>5</sup> Au(I) alkynylphosphine complexes [(MeO(C<sub>6</sub>H<sub>4</sub>))<sub>3</sub>P–Au–C $\equiv$ C–R] (R = phenyl, 2-thienyl or 4-(thiophen-2-yl)phenyl) were obtained from the phosphine chloride precursor [(MeO(C<sub>6</sub>H<sub>4</sub>))<sub>3</sub>P–AuCl] by a simple procedure<sup>6</sup> involving an interaction with the corresponding terminal alkyne in the presence of NaOAc/NEt<sub>3</sub>. The alkynylcarbene derivative [(iPr)<sub>2</sub>bIm–Au–C $\equiv$ C–Ph] was synthesised according to the literature protocol.<sup>7</sup>

### Synthesis of POV precursor

(Bu<sub>4</sub>N)<sub>2</sub>[V<sub>6</sub>O<sub>13</sub>{(OCH<sub>2</sub>)<sub>3</sub>CCH<sub>2</sub>-N<sub>3</sub>}<sub>2</sub>] ({V<sub>6</sub>}-N<sub>3</sub>). The title compound was synthesised according to the adopted classical method.<sup>8,9</sup> (Bu<sub>4</sub>N)<sub>3</sub>[H<sub>3</sub>V<sub>10</sub>O<sub>28</sub>] (1.69 g, 1.0 mmol) was dissolved in 50 mL MeCN together with (HO-CH<sub>2</sub>)<sub>3</sub>C-CH<sub>2</sub>-N<sub>3</sub> (488 mg, ca. 3 mmol) and refluxed for 24 hrs. The resulting dark clear solution was cooled to room temperature and 28 mL diethyl ether was added. The resulting system was let to stay for three days, affording the orange crystals, which were filtered off, washed with ethanol (3x5 mL), and dried *in vacuo*. Yield: 480 mg (36%). NMR and ESI-MS data are in accordance with previously published ones<sup>10</sup>.

### Synthesis of {V<sub>6</sub>}-organogold hybrids

**(Bu<sub>4</sub>N)<sub>2</sub>[V<sub>6</sub>O<sub>13</sub>{(OCH<sub>2</sub>)<sub>3</sub>CCH<sub>2</sub>(N<sub>3</sub>C<sub>2</sub>Ph)AuP(C<sub>6</sub>H<sub>4</sub>OMe)<sub>3</sub>}<sub>2</sub>] (1).** A 50 ml reaction flask was degassed, filled with argon and charged with {V<sub>6</sub>}-N<sub>3</sub> (120 mg, 0.091 mmol), (MeO(C<sub>6</sub>H<sub>4</sub>))<sub>3</sub>PAuC≡CPh (130 mg, 0.2 mmol), 17 mL of a freshly purified degassed DMF, CuI (20 mg, 0.105 mmol), and N,N-diisopropylethylamine (40 μL). The solution was degassed again and stirred at 60°C for 1 hour within the microwave treatment (250 W). The resulting solution was passed through a pad of neutral alumina and a pad of celite, evaporated *in vacuo* to ca. 0.5 ml, diluted with 2 ml of CH<sub>2</sub>Cl<sub>2</sub> and poured into 10 ml of Et<sub>2</sub>O. The precipitate was collected by centrifugation, re-dissolved in 3 mL of CH<sub>2</sub>Cl<sub>2</sub> and then precipitated with NEt<sub>3</sub>. The precipitate was washed (4 ml of MeOH, 10 mL of Et<sub>2</sub>O) and dried *in vacuo*. The resulting product was purified by preparative SEC with Sephadex LH-20 in a DMF media. Yield: 126 mg (53%). NMR and ESI-MS data are in accordance with published ones.<sup>11</sup>

**(Bu<sub>4</sub>N)<sub>2</sub>[V<sub>6</sub>O<sub>13</sub>{(OCH<sub>2</sub>)<sub>3</sub>CCH<sub>2</sub>(N<sub>3</sub>C<sub>2</sub>Ph)Au-bIm(iPr)<sub>2</sub>}<sub>2</sub>] (2).** The title compound was obtained according to the method described for **1**. The synthesis started from 62 mg {V<sub>6</sub>}-N<sub>3</sub> (0.047 mmol) and 59 mg [(iPr)<sub>2</sub>bIm-Au-C≡C-Ph] (0.117 mmol). 50 mg (Yield: 46%) of **2** was obtained as yellowish orange powder. <sup>1</sup>H NMR (400 MHz, DMSO-*d*<sub>6</sub>) δ 8.24 (d, *J* = 7.9 Hz, 4H), 7.98 (m, 4H), 7.44 (m, 4H), 7.36 (t, *J* = 7.4 Hz, 4H), 7.23 (t, *J* = 6.3 Hz, 2H), 5.48 (hept, *J* = 6.1 Hz, 4H), 5.04 (s, 12H), 4.44 (s, 4H), 3.17 (m, 16H), 1.70 (d, *J* = 6.9 Hz, 24H), 1.57 (m, 16H), 1.32 (m, 16H), 0.94 (t, *J* = 7.2 Hz, 24H). ESI<sup>-</sup> MS *m/z*: [M]<sup>2-</sup> found 915.0115, calcd. 915.0087; [M+O]<sup>2-</sup> found 923.0122, calcd. 923.0061, where M = [C<sub>52</sub>H<sub>62</sub>Au<sub>2</sub>N<sub>10</sub>O<sub>19</sub>V<sub>6</sub>].

**(Bu<sub>4</sub>N)<sub>2</sub>[V<sub>6</sub>O<sub>13</sub>{(OCH<sub>2</sub>)<sub>3</sub>CCH<sub>2</sub>(N<sub>3</sub>C<sub>2</sub>(C<sub>6</sub>H<sub>4</sub>-thyenyl))AuP(C<sub>6</sub>H<sub>4</sub>OMe)<sub>3</sub>}<sub>2</sub>] (3).** The title compound was obtained according to the method described for **1**. The synthesis started from 54 mg {V<sub>6</sub>}-N<sub>3</sub> (0.041 mmol) and 75 mg [(MeO(C<sub>6</sub>H<sub>4</sub>))<sub>3</sub>P-Au-C≡C-(C<sub>6</sub>H<sub>4</sub>-thyenyl)] (0.102 mmol). 34,5 mg (Yield: 30%) of **3** was obtained as orange powder. <sup>1</sup>H NMR (400 MHz, DMSO-*d*<sub>6</sub>) δ 8.17 (d, *J* = 7.6 Hz, 4H), 7.53 – 7.46 (m, 20H), 7.20 (d, *J* = 7.3 Hz, 12H), 7.15 (dd, *J* = 5.0, 3.7 Hz, 2H), 5.08 (s, 12H), 4.44 (s, 4H), 3.87 (s, 18H), 3.17 (m, 16H), 1.57 (m, 16H), 1.32 (m, 16H), 0.94 (t, *J* = 7.3 Hz, 24H). <sup>31</sup>P NMR (162 MHz, DMSO-*d*<sub>6</sub>) δ 39.65. ESI<sup>-</sup> MS *m/z*: [M]<sup>2-</sup> found 1146.9750, calcd. 1146.9722; [M+O]<sup>2-</sup> found 1154.9714, calcd. 1154.9697, where M = [C<sub>76</sub>H<sub>72</sub>Au<sub>2</sub>N<sub>6</sub>O<sub>25</sub>P<sub>2</sub>S<sub>2</sub>V<sub>6</sub>].

**(Bu<sub>4</sub>N)<sub>2</sub>[V<sub>6</sub>O<sub>13</sub>{(OCH<sub>2</sub>)<sub>3</sub>CCH<sub>2</sub>(N<sub>3</sub>C<sub>2</sub>(thyenyl))AuP(C<sub>6</sub>H<sub>4</sub>OMe)<sub>3</sub>}<sub>2</sub>] (4).** The title compound was obtained according to the method described for **1**. The synthesis started from 71 mg {V<sub>6</sub>}-N<sub>3</sub> (0.054 mmol) and 85 mg [(MeO(C<sub>6</sub>H<sub>4</sub>))<sub>3</sub>P-Au-C≡C-(thyenyl)] (0.13 mmol). 74 mg (Yield: 52%) of the **4** was obtained as yellowish orange powder. <sup>1</sup>H NMR (400 MHz, DMSO-*d*<sub>6</sub>) δ 7.55 – 7.46 (m, 14H), 7.26 (d, *J* = 4.6 Hz, 2H), 7.18 (d, *J* = 7.2 Hz, 12H), 6.98 (dd, *J* = 4.9, 3.6 Hz, 2H), 5.04 (s, 12H), 4.38 (s, 4H), 3.87 (s, 18H), 3.17 (m, 16H), 1.57 (m, 16H), 1.31 (m, 16H), 0.93 (t, *J* = 7.3 Hz, 24H). <sup>31</sup>P NMR (162

MHz, DMSO- $d_6$ )  $\delta$  39.64. ESI<sup>-</sup> MS  $m/z$ :  $[M]^{2-}$  found 1070.9403, calcd. 1070.9409;  $[M+O]^{2-}$  found 1078.9377, calcd. 1078.9384, where  $M = [C_{64}H_{64}Au_2N_6O_{25}P_2S_2V_6]$ .

### STM/STS measurements and sample preparation

The solutions of  $\{V_6\}$ -Au hybrids in  $CH_2Cl_2$  or acetonitrile were passed through a PTFE 0.22  $\mu m$  filter and used for drop casting immediately after preparation. The drops of the volume 1.5 – 2  $\mu l$  ( $c = 10^{-4}$  M or  $10^{-5}$  M) were deposited on the epitaxial Au(111)/mica surface and placed into a high vacuum load chamber of the STM machine.

STM and STS experiments were conducted under ultra-high-vacuum (UHV) conditions at room temperature in a Scienta Omicron VT-SPM instrument. The base pressure inside the stainless-steel vessel during operation was  $2 \times 10^{-9}$  mbar. For all measurements, commercial Pt tips from Bruker were used. All images were measured in constant current mode. Most images were obtained by using a bias voltage +1 V and a tunneling set point of 10 pA, some specific cases with different bias voltages are noted individually. The applied bias voltage is always referred to the substrate, thus, the STM tip is set to negative polarity. Voltage sweep rate for STS measurements was 588 mV/s.

Since a single STS  $I(V)$  measurement typically suffers from a great variety of uncontrolled factors (e.g., needle position drift, bad electric contact, change of the needle tip conditions in the course of the measurements, electrostatic interactions, etc.), the single  $I(V)$  curve could not be considered reliable. That is why we measured them plenty of times in different positions and calculated the average  $I(V)$  curves for the set of manually preselected data. To validate the data reliability, the average curves obtained for independent data sets were compared.

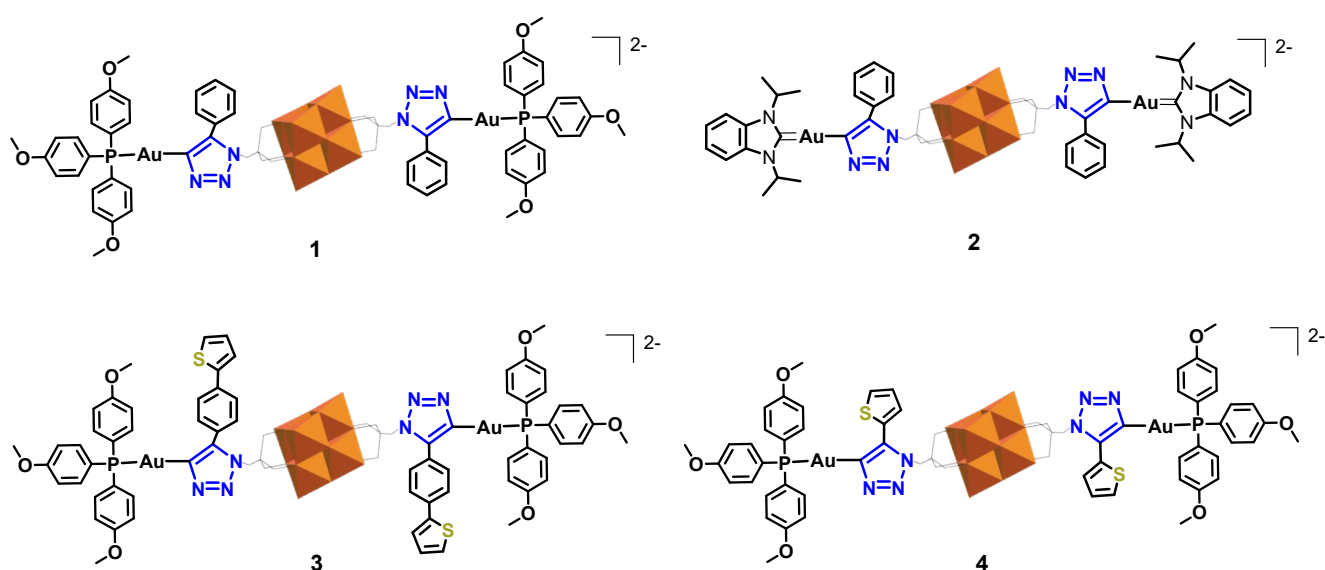


**Figure S1.** The structures of compounds 1–4 ( $NBu_4^+$  cations omitted).

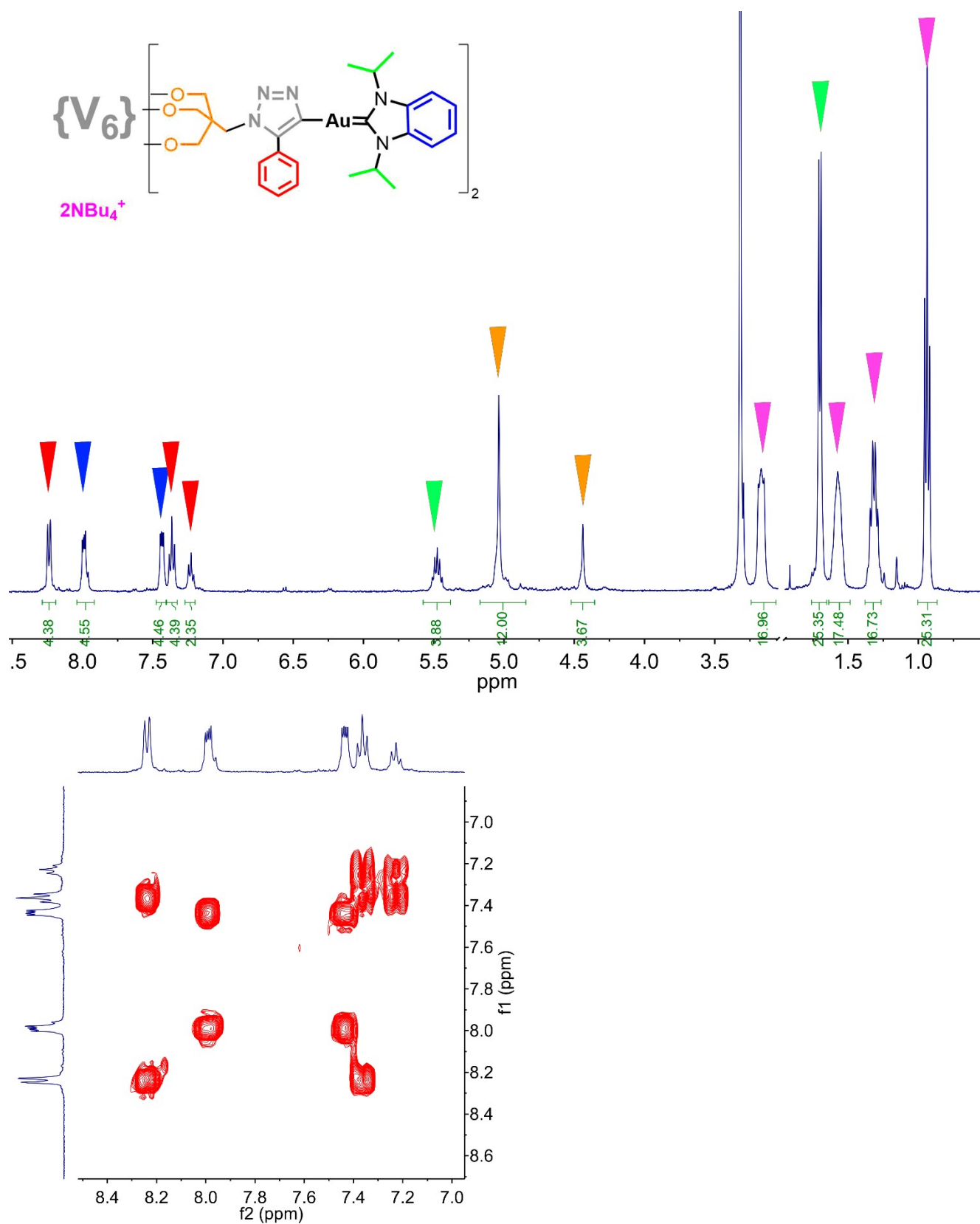


**Figure S2.**  $^1H$  NMR (top) and  $^1H$ - $^1H$  COSY NMR (aromatic region, bottom) spectra of hybrid 2.

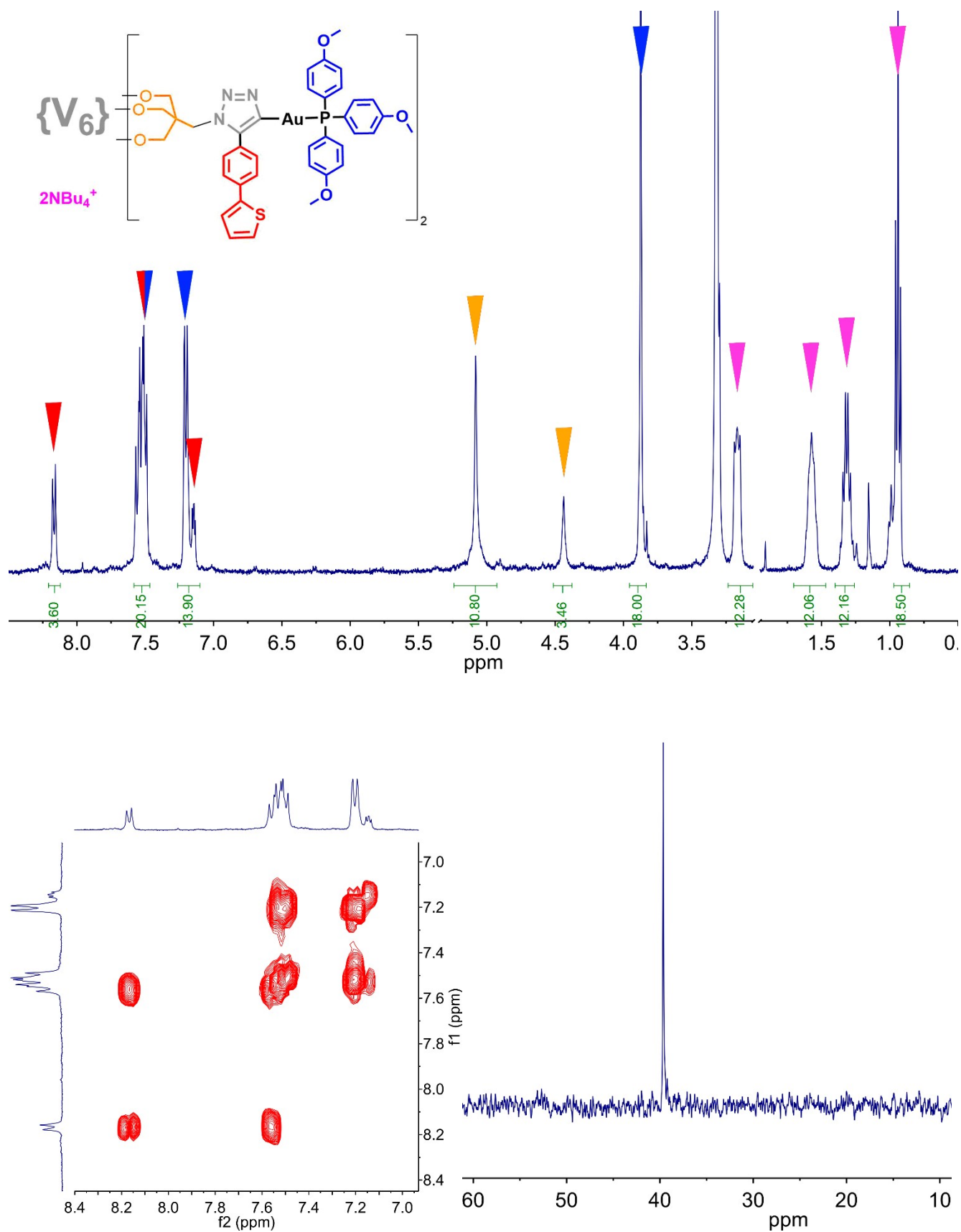


**Figure S3.**  $^1H$  NMR (top),  $^1H$ - $^1H$  COSY NMR (aromatic region, bottom left) and  $^{31}P$  NMR (bottom right) of hybrid 3.



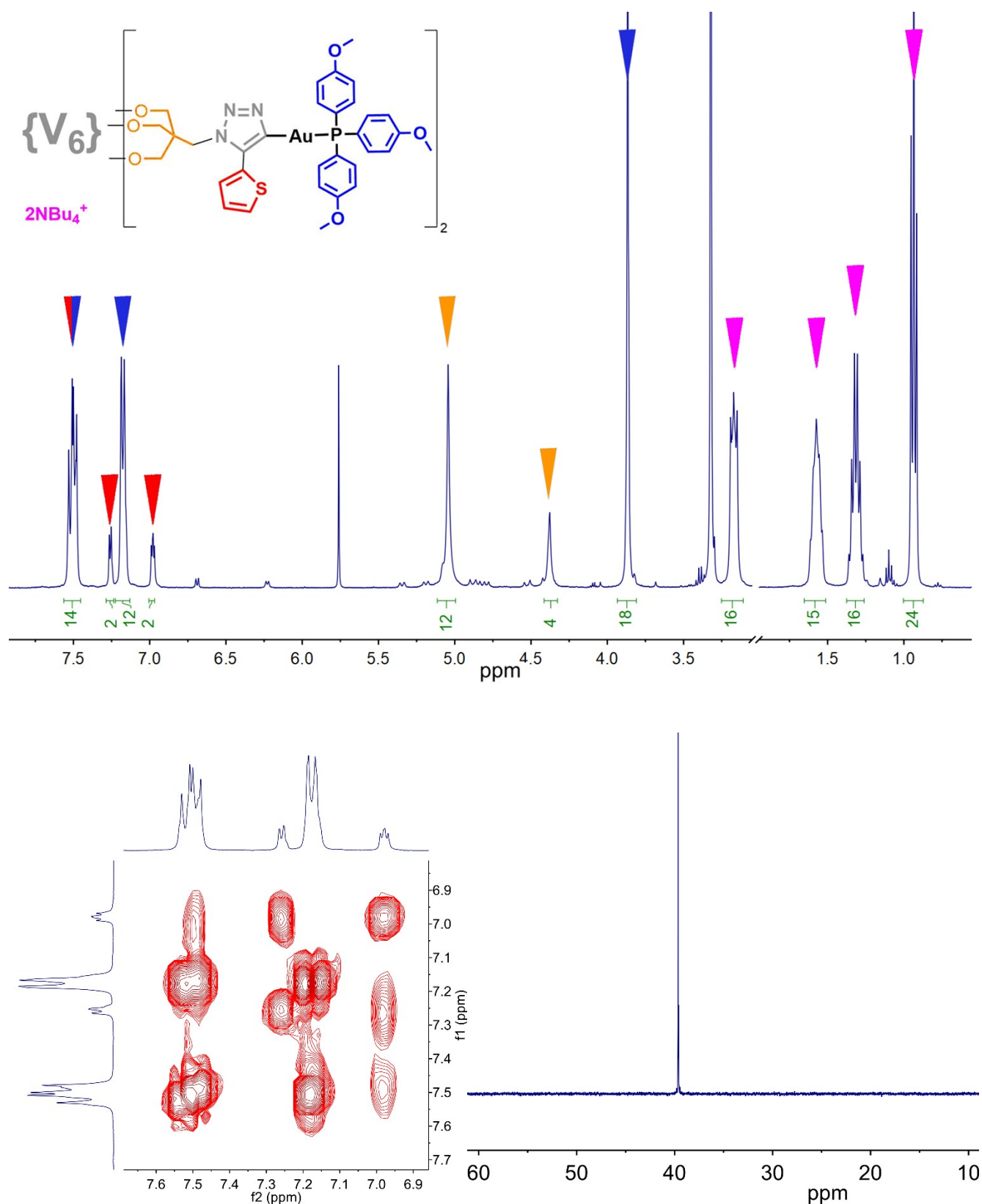


**Figure S4.** <sup>1</sup>H NMR (top), <sup>1</sup>H-<sup>1</sup>H COSY NMR (aromatic region, bottom left) and <sup>31</sup>P NMR (bottom right) of hybrid 4.

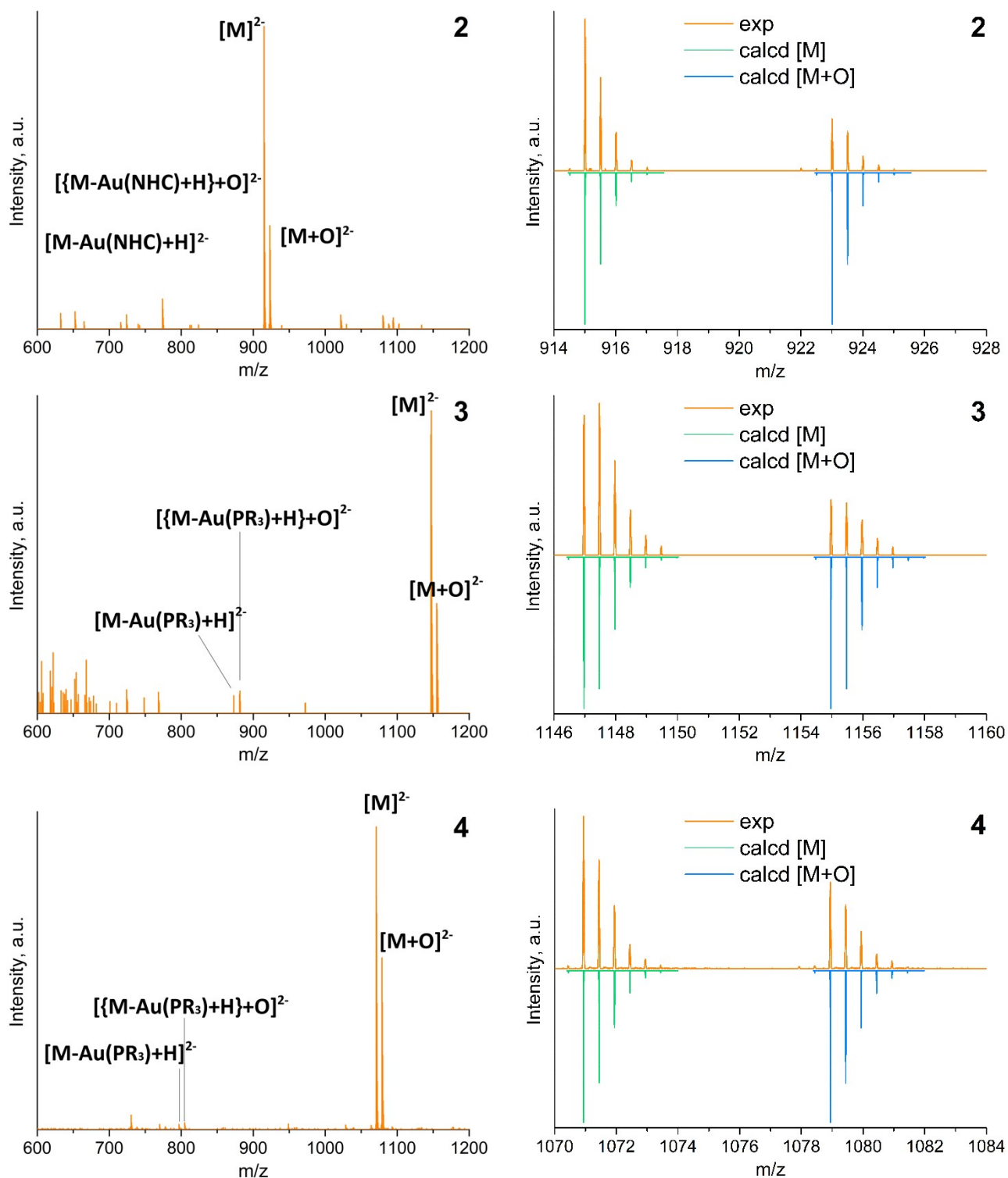


**Figure S5.** ESI-MS of  $\{V_6\}$ -Au: experimental spectrum and simulated isotopic patterns for the dominating signals.

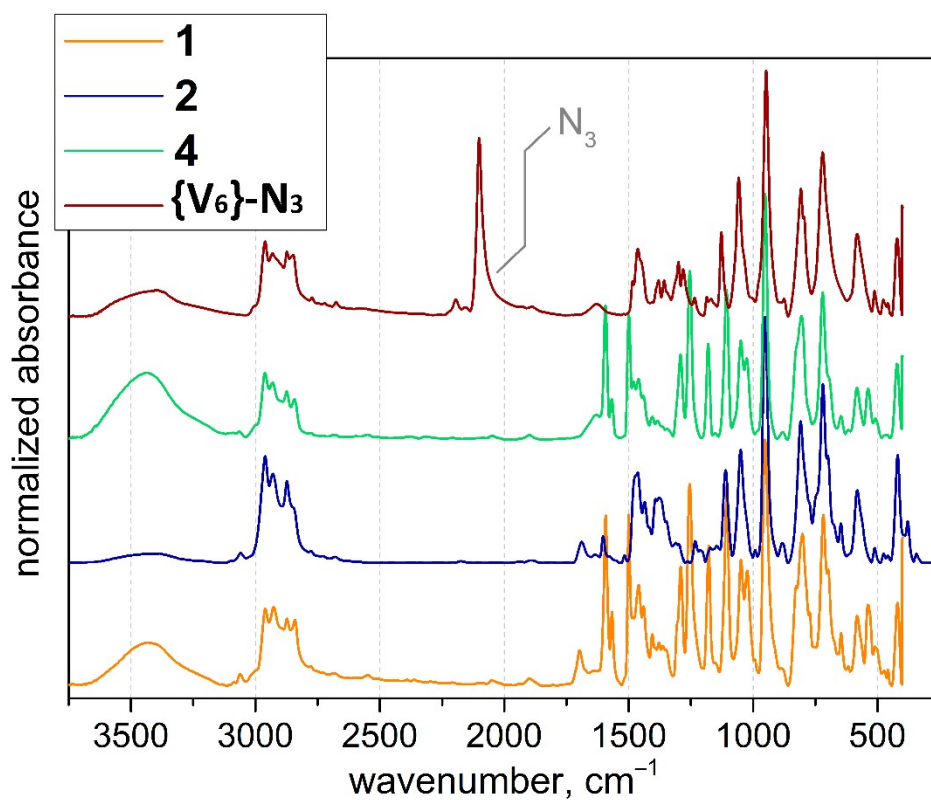


**Figure S6.** FTIR spectra of hybrids  $\{\text{V}_6\}\text{-Au}$  and  $\{\text{V}_6\}\text{-N}_3$  in the fingerprint region, KBr.

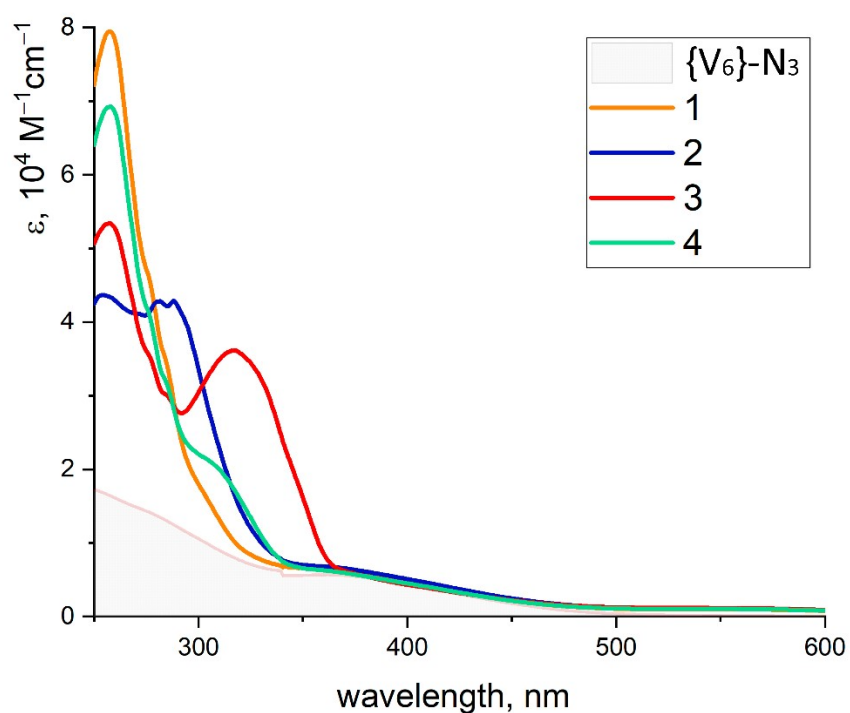


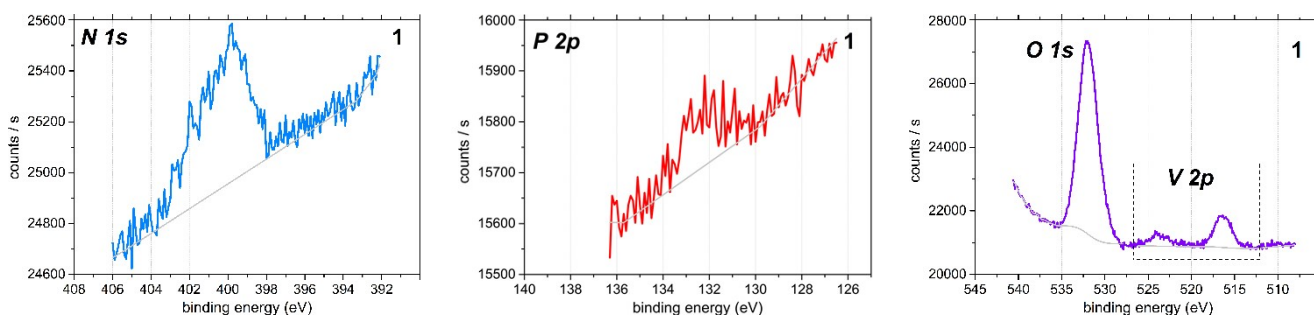
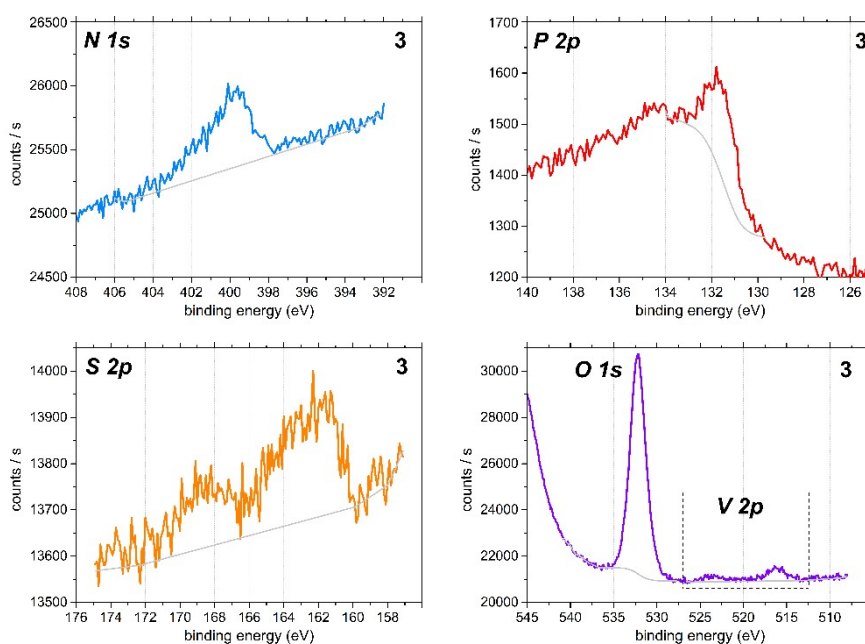
**Figure S7.** UV-vis absorption spectra of the hybrids 1–4 and  $\{\text{V}_6\}\text{-N}_3$  (for comparison) in  $10^{-5} \text{ M}$   $\text{CH}_2\text{Cl}_2$  solutions.

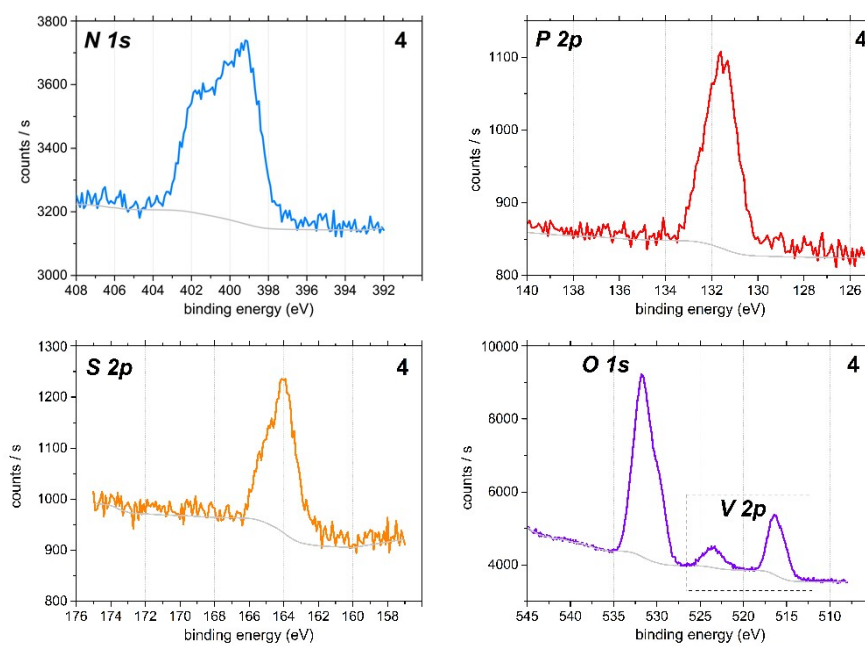
**Table S1.** Binding energy of element signals observed in XPS spectra of **1**, **3** and **4**.

	<b>1</b>	<b>3</b>	<b>4</b>
<b>N 1s</b>	399.8	399.8	399.7; 401.6
<b>P 2p</b>	131.7*	131.8*	131.5*
<b>O 1s</b>	532.0	532.2	531.8
<b>V 2p</b>	523.9 (V 2p <sub>1/2</sub> ); 516.4 (V 2p <sub>3/2</sub> )	523.9 (V 2p <sub>1/2</sub> ); 516.4 (V 2p <sub>3/2</sub> )	523.7 (V 2p <sub>1/2</sub> ); 516.4 (V 2p <sub>3/2</sub> )
<b>S 2p</b>	–	168.2*†; 162.0*	164.1

\* Centre of the signal

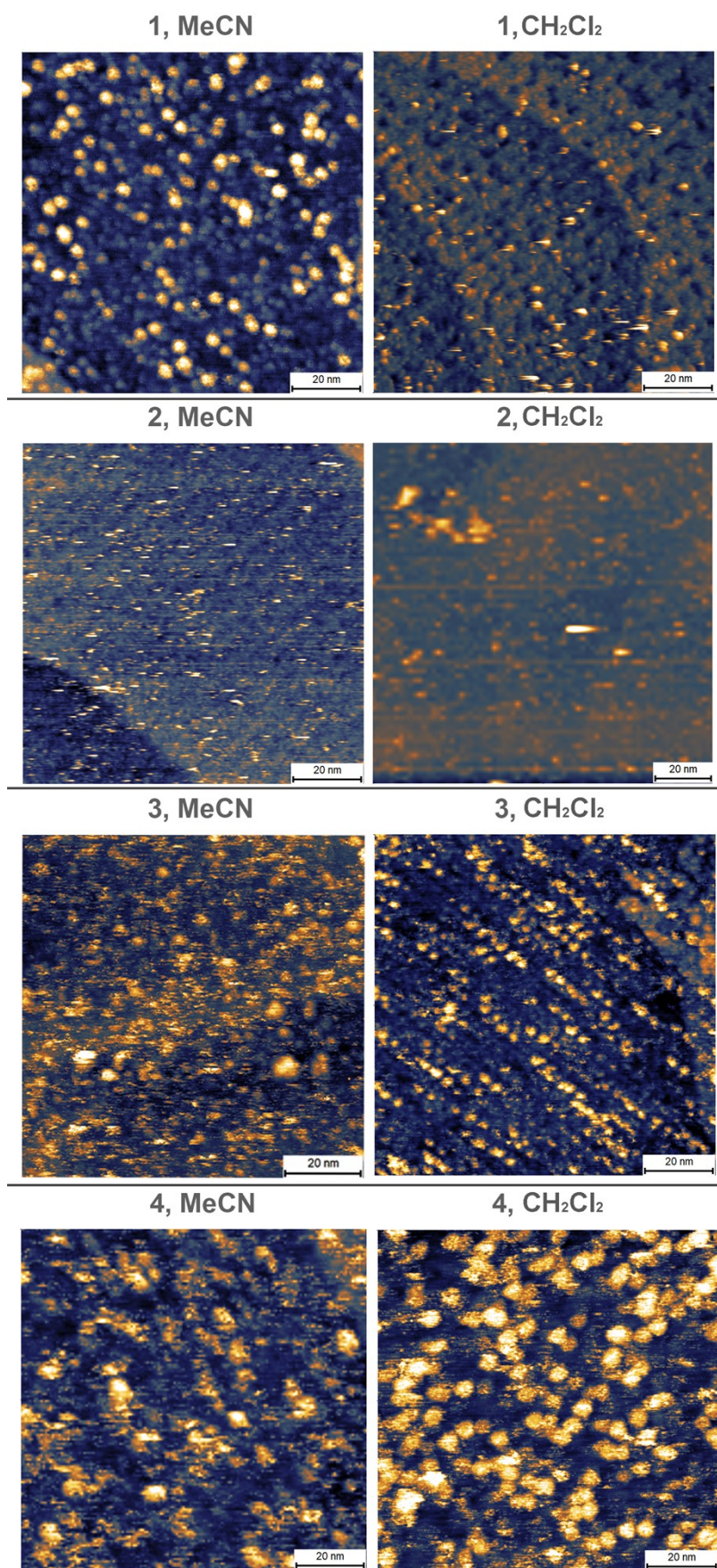
† The signal is attributed to oxidated Sulphur, which is originated from oxidation of the Au-S moieties at ambient conditions,<sup>12</sup> until the samples were place in UHV chamber of XPS machine.

**Figure S8.** Photoemission core-level N 1s, P 2p, O 1s and V 2p spectra taken from freshly deposited molecular layers of complex **1** on Au(111).**Figure S9.** Photoemission core-level N 1s, S 2p, O 1s and V 2p spectra taken from freshly deposited molecular layers of complex **3** on Au(111), and P 2p on Si.

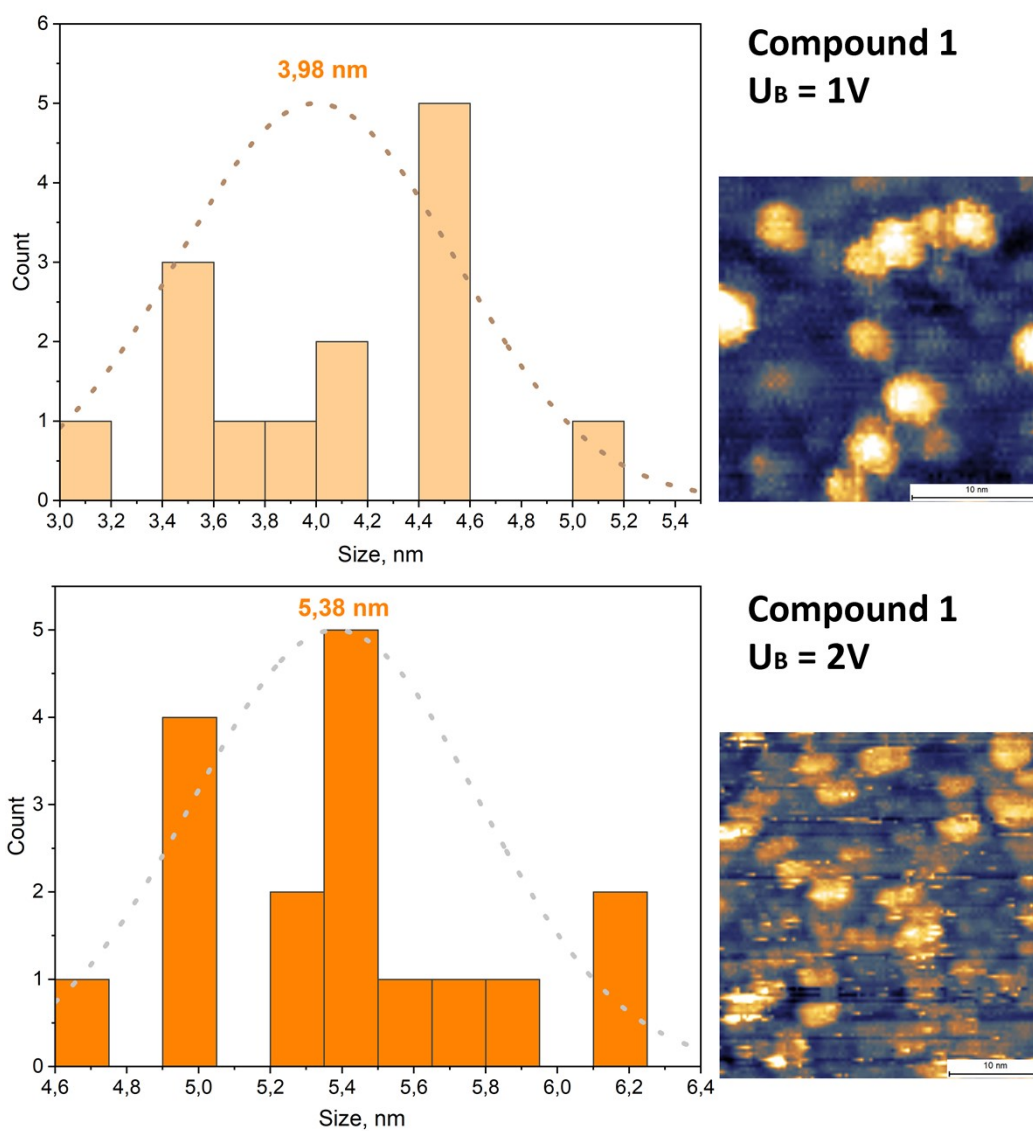


**Figure S10.** Photoemission core-level N 1s, P 2p, S 2p, O 1s and V 2p spectra taken from freshly deposited molecular layers of complex 4 on Au(111).

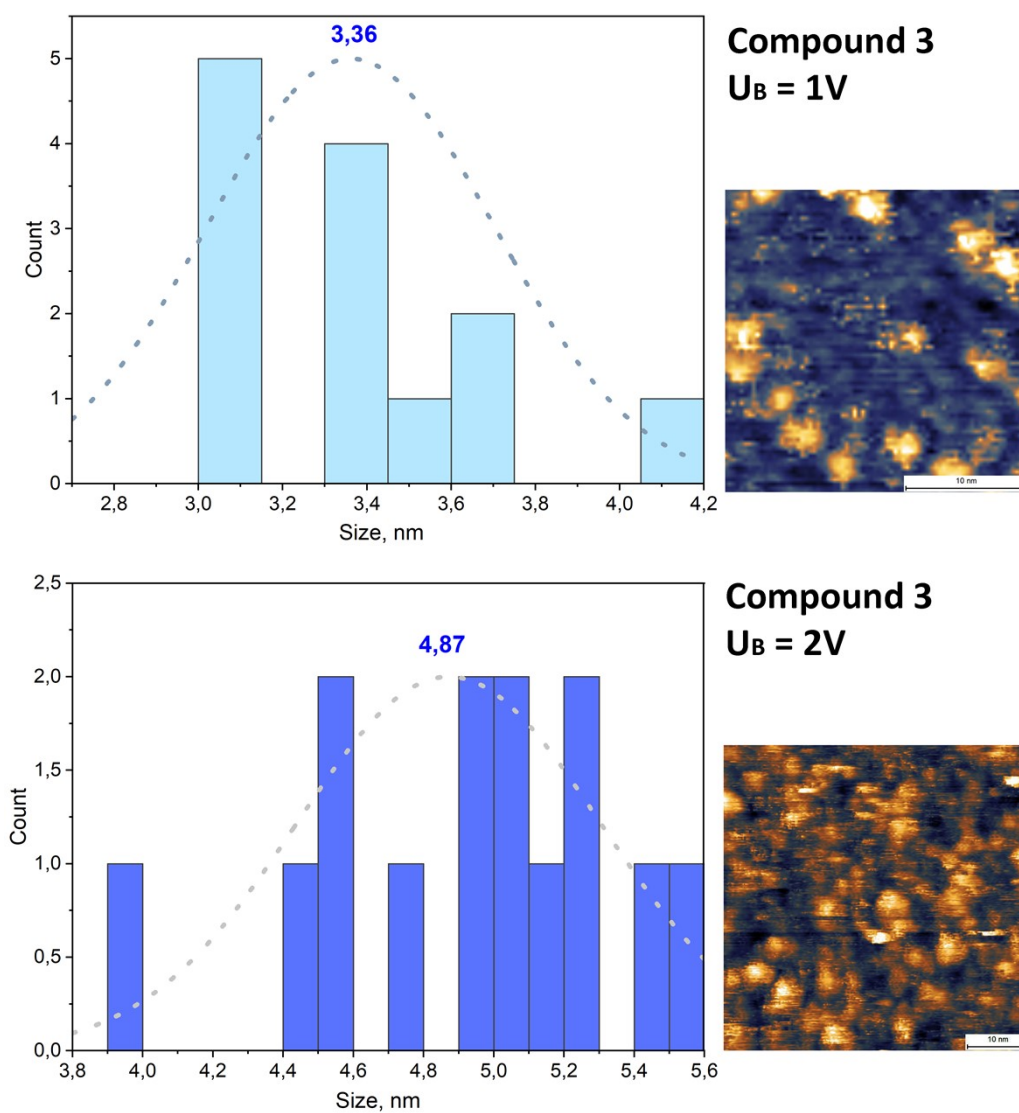




**Figure S11.** STM images ( $U_B = 1$  V;  $I_T = 10$  pA) of the samples obtained by drop casting deposition of  $10^{-5}$  M MeCN and CH<sub>2</sub>Cl<sub>2</sub> solutions of **1–4** on Au(111).

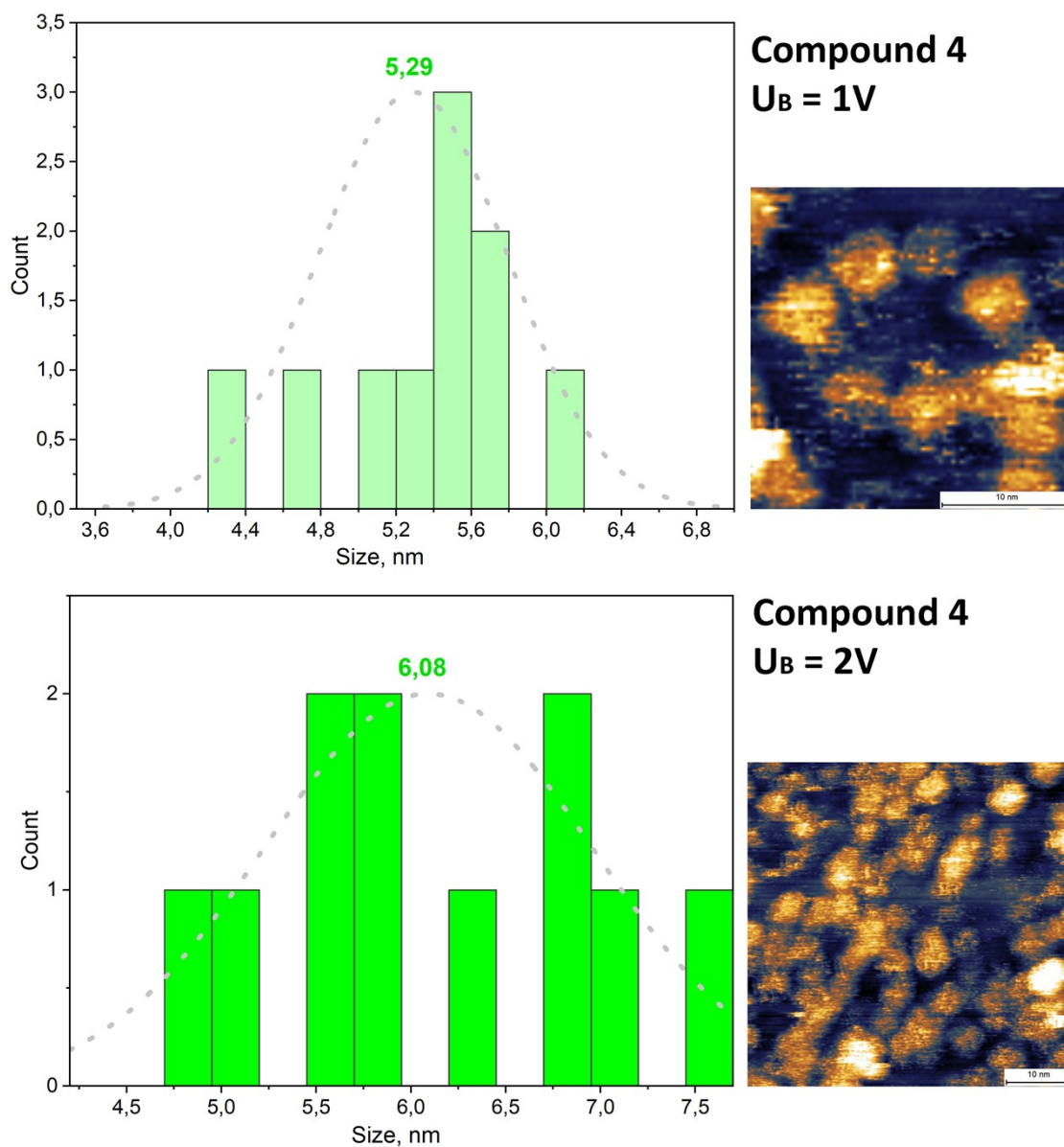


**Figure S12.** Particle size distribution observed at different  $U_B$  values for the selected area of the samples obtained by drop casting deposition of **1** onto the Au(111) surface. The normal distribution fitting is applied to estimate the average particle sizes.

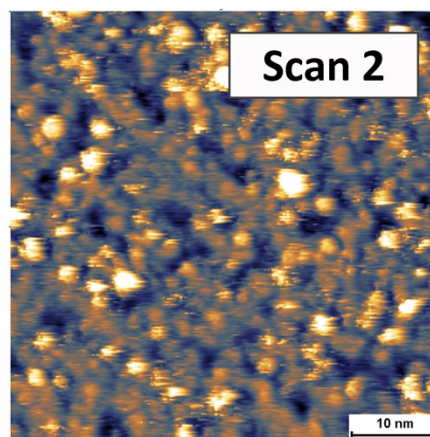
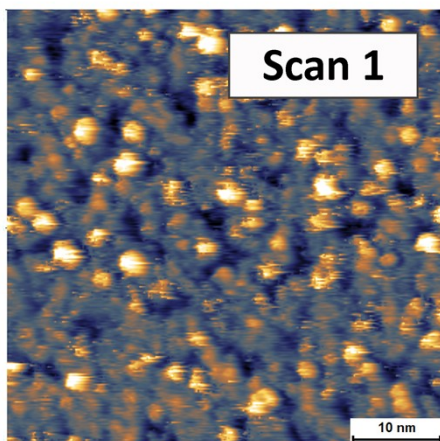
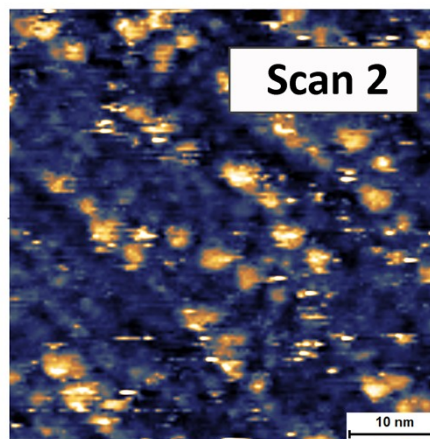
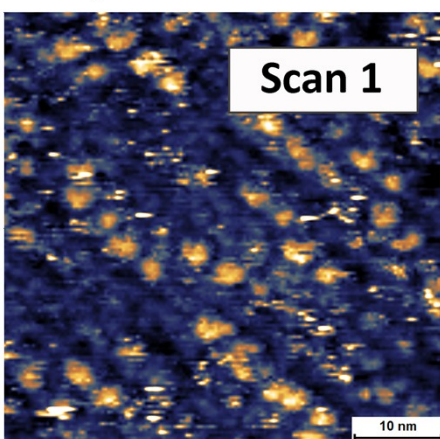
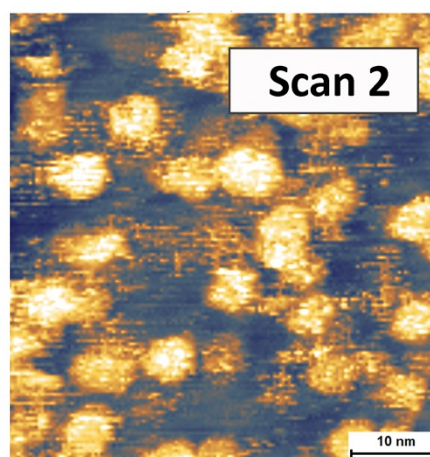
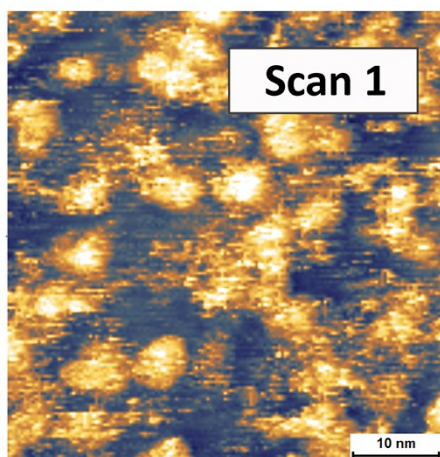


**Figure S13.** Particle size distribution observed at different  $U_B$  values for the selected area of the samples obtained by drop casting deposition of **3** onto the Au(111) surface. The normal distribution fitting is applied to estimate the average particle sizes.





**Figure S14.** Particle size distribution observed at different  $U_B$  values for the selected area of the samples obtained by drop casting deposition of **4** onto the Au(111) surface. The normal distribution fitting is applied to estimate the average particle sizes.

**Compound 1****Compound 3****Compound 4**

**Figure S15.** Subsequent STM scans ( $U_B = 1$  V;  $I_T = 10$  pA) for compounds 1, 3, and 4.

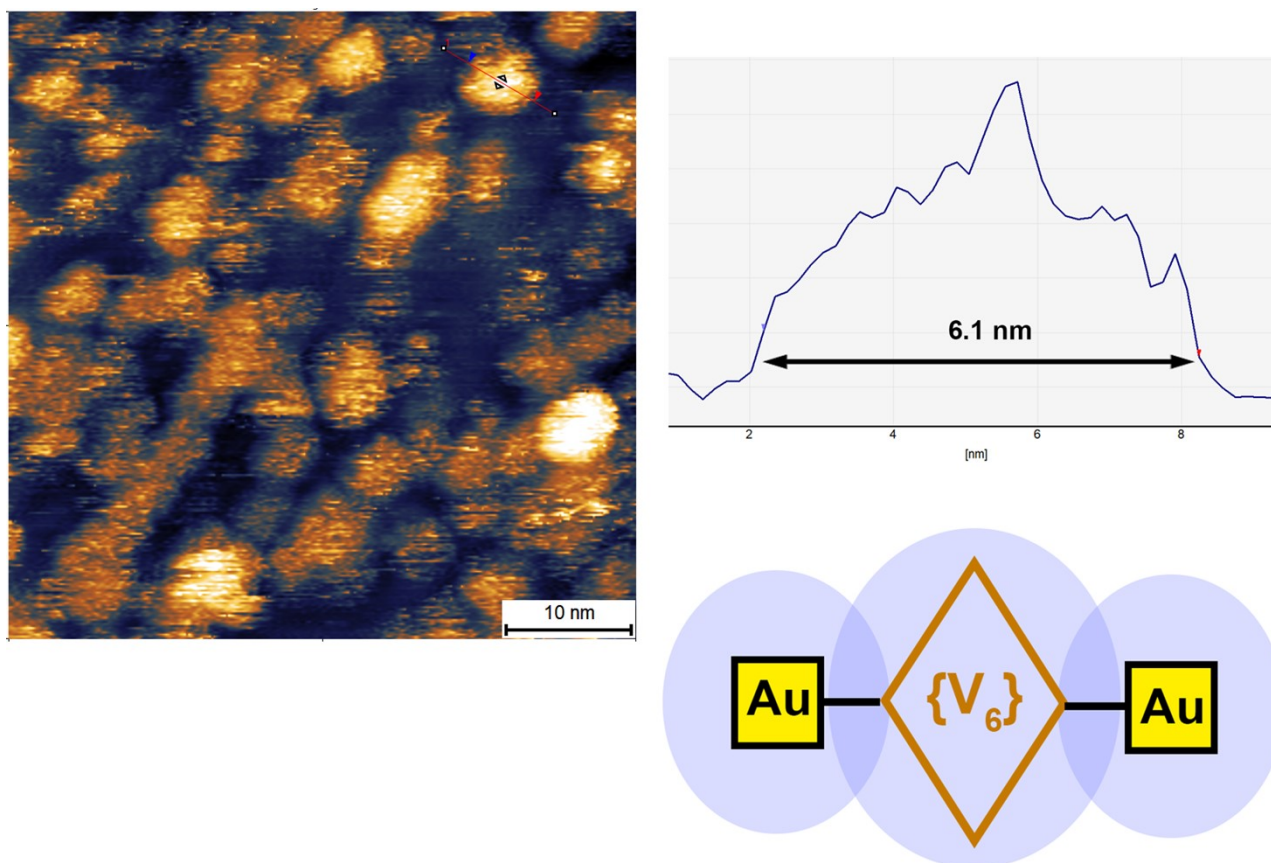


**Figure S16.** STM image ( $U_B = 2$  V;  $I_T = 10$  pA) of **4** on Au(111). Cross-section of one particle and schematic representation of possible charge distribution.

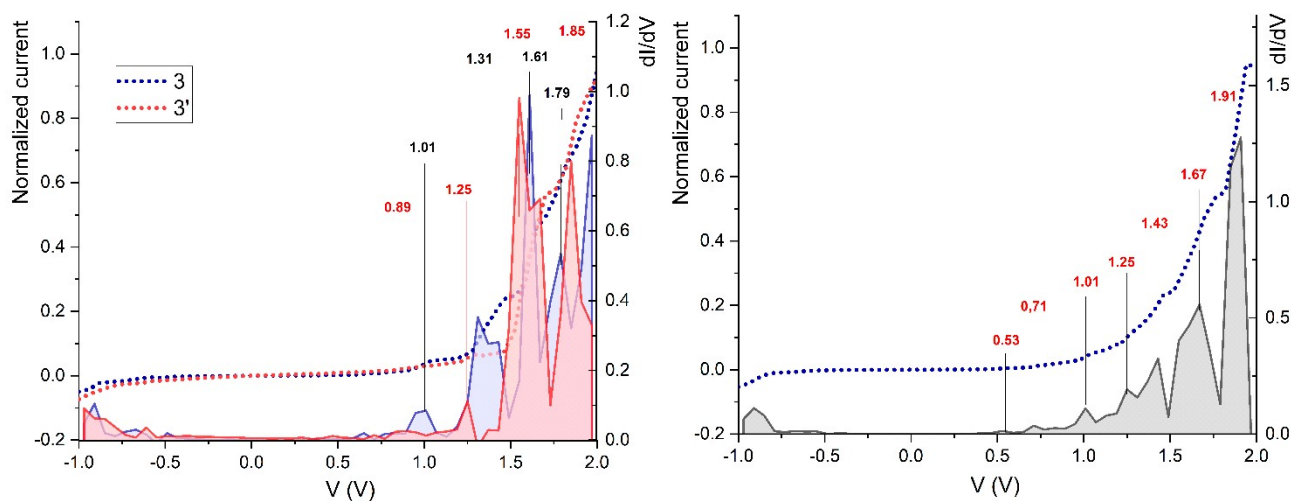


**Figure S17.** STS  $I(V)$  curves (dashed) and derivative  $dI/dV$  (solid) curves for single molecules of **3** (left) and **4** (right) on Au(111). The data were obtained as average for the set of 47 selected  $I(V)$  curves (**4**) and two sets containing 35 (blue line) and 12 (red line) curves. The very poor data convergency for **3** illustrates destabilization of its reduced states on Au(111).

**References**

1. W. L. F. Armarego and C. L. L. Chai, *Purification of Laboratory Chemicals*, 2013.
2. O. V. Starikova, G. V. Dolgushin, L. I. Larina, T. N. Komarova and V. A. Lopyrev, *Arkivoc*, 2003, **2003**, 119-124.
3. L. Zheng, Q. Jiang, H. Bao, B. Zhou, S.-P. Luo, H. Jin, H. Wu and Y. Liu, *Org. Lett.*, 2020, **22**, 8888-8893.
4. R. Uson, A. Laguna, M. Laguna, D. A. Briggs, H. H. Murray and J. P. Fackler, *Inorg. Synth.*, 2007, **29**, 85-91.
5. G. E. Coates and C. Parkin, *J. Chem. Soc.*, 1962, 3220-3226.
6. S. Petrovskii, A. Senchukova, V. Sizov, A. V. Paderina, M. Luginin, E. Abramova and E. V. Grachova, *Mol. Syst. Des. Eng.*, 2022, **7**, 1249-1262.
7. J. A. Garg, O. Blacque, J. Heier and K. Venkatesan, *Eur. J. Inorg. Chem.*, 2012, **2012**, 1750-1763.
8. Q. Chen, D. P. Goshorn, C. P. Scholes, X. L. Tan and J. Zubieta, *J. Am. Chem. Soc.*, 2002, **114**, 4667-4681.
9. O. Linnenberg, A. Kondinski, C. Stöcker and K. Y. Monakhov, *Dalton Trans.*, 2017, **46**, 15636-15640.
10. H. Jia, Q. Li, A. Bayaguud, Y. Huang, S. She, K. Chen and Y. Wei, *Dalton Trans.*, 2018, **47**, 577-584.
11. S. K. Petrovskii, V. V. Khistiaeva, A. A. Sizova, V. V. Sizov, A. V. Paderina, I. O. Koshevoy, K. Y. Monakhov and E. V. Grachova, *Inorg. Chem.*, 2020, **59**, 16122-16126.
12. T. M. Willey, A. L. Vance, T. van Buuren, C. Bostedt, L. J. Terminello and C. S. Fadley, *Surf. Sci.*, 2005, **576**, 188-196.